RESEARCH PAPER

Exploring Cissus Verticillata as a Source of HER2 Inhibitors: Phytochemical Profiling, Molecular Docking, and ADMET Analysis

Chiripireddy Saichandana[1], P. Dharani Prasad[1]*

[1]*Department of Pharmacology, School of Pharmaceutical Sciences (Erstwhile Sree Vidyaniketan College of Pharmacy), Mohan Babu University, Tirupati 517102, Andhra Pradesh, India*

Received: 11th Aug, 2025; Revised: 10th Sep 2025; Accepted: 16th Nov, 2025; Available Online: 30th Nov, 2025

ABSTRACT

Cissus verticillata, a traditionally valued medicinal plant, was investigated for its phytochemical composition and therapeutic potential through integrated experimental and computational approaches. The plant material was authenticated, extracted with hydroalcoholic solvent, and subjected to organoleptic, physicochemical, microbial, and phytochemical analyses. The extract yield was 10.95%, appearing dark brown to greenish-brown with stable physicochemical parameters, near-neutral pH, and absence of microbial or heavy metal contamination. Preliminary phytochemical screening confirmed abundant flavonoids, phenolics, and alkaloids, with moderate tannins and saponins, highlighting strong antioxidant and anti-inflammatory potential. LC-HRMS profiling revealed a chemically diverse fingerprint, with seven major compounds tentatively identified: kaempferol-3-O-rutinoside, rutin, chlorogenic acid, luteolin-7-O-glucoside, procyanidin B2, a saponin derivative, and cinnamtannin A2. These metabolites represent key classes of flavonoids, phenolic acids, tannins, and saponins. Molecular docking against the HER2 enzyme (PDB ID: 3RCD) revealed promising binding affinities, with rutin (-10.3 kcal/mol), kaempferol-3-O-rutinoside (-10.2 kcal/mol), and luteolin-7-O-glucoside (-9.9 kcal/mol) surpassing the native ligand (-9.6 kcal/mol). These compounds formed multiple hydrogen bonds with residues such as MET801, ASP863, and ARG849, along with hydrophobic interactions that stabilized binding. Procyanidin B2 (-9.2 kcal/mol) and soyasaponin I (-9.1 kcal/mol) showed moderate affinity, while chlorogenic acid (-8.2 kcal/mol) and cinnamtannin A2 (-6.2 kcal/mol) exhibited lower activity. In silico ADMET predictions confirmed that chlorogenic acid, luteolin-7-O-glucoside, and kaempferol-3-O-rutinoside possessed superior drug-likeness, good absorption, minimal CYP450 interaction, and reduced toxicity compared to the native ligand. These findings support *Cissus verticillata* as a phytochemical-rich candidate for HER2-targeted therapeutic development.

Keywords: Cissus verticillata, LC-HRMS, phytoconstituents, HER2, molecular docking, ADMET.

How to cite this article: Saichandana C, Prasad PD. Exploring Cissus verticillata as a Source of HER2 Inhibitors: Phytochemical Profiling, Molecular Docking, and ADMET Analysis. Int J Drug Deliv Technol. 2025;15(4): 1514-1532, DOI: 10.25258/ijddt.15.4.8.

Source of support: Nil.

Conflict of interest: None

INTRODUCTION

Cancer continues to be a major global health challenge, representing one of the leading causes of morbidity and mortality. Among the diverse forms of cancer, breast cancer remains the most prevalent, accounting for millions of new cases each year worldwide[1,2]. A significant proportion of breast cancers are characterized by the overexpression of the Human Epidermal Growth Factor Receptor 2 (HER2), a transmembrane tyrosine kinase receptor that plays a pivotal role in cell proliferation, survival, and metastasis. HER2-positive breast cancers are often associated with aggressive disease progression, resistance to conventional therapies, and poorer prognoses compared with HER2-negative cases. The clinical success of HER2-targeted therapies, such as trastuzumab and lapatinib, underscores the therapeutic relevance of this receptor. However, issues including acquired resistance, adverse side effects, and limited accessibility of synthetic drugs highlight the urgent need to explore alternative, safer, and more sustainable HER2 inhibitors[3,4,5,6,7].

In this context, natural products derived from medicinal plants have gained increasing attention in modern drug discovery. Plants synthesize a remarkable diversity of secondary metabolites, many of which serve as chemical defenses against pathogens and environmental stresses but also exhibit potent pharmacological activities in humans. Phytochemicals such as flavonoids, alkaloids, tannins, saponins, and phenolic acids are well-documented for their antioxidant, anti-inflammatory, and anticancer properties[8,9,10,11,12].Importantly, numerous plant-derived compounds have already contributed to the development of anticancer drugs, including paclitaxel, vincristine, and camptothecin. The structural complexity, bioactivity, and relative safety of phytoconstituents make them valuable candidates for screening against molecular targets such as HER2. Among the wide spectrum of medicinal plants, *Cissus verticillata* (L.), a member of the Vitaceae family, has emerged as a botanically and pharmacologically significant species. Commonly referred to as “Princess Vine” or “Season Vine,”

**Author for Correspondence: dharaniprasadp@gmail.com*

GRAPHICAL ABSTRACT

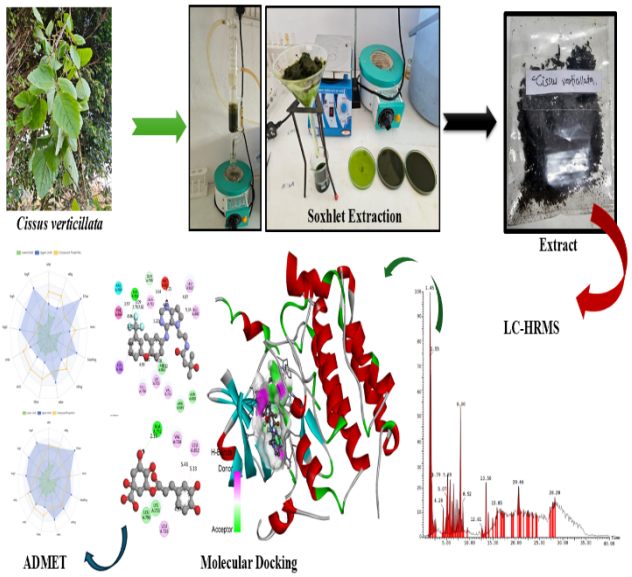

it is widely distributed in tropical and subtropical regions. Traditionally, the plant has been employed in various ethnomedicinal practices for managing ailments such as inflammation, gastrointestinal disturbances, diabetes, and infections. Preliminary studies suggest that Cissus species are rich in flavonoids, stilbenes, tannins, and other polyphenolic compounds, many of which have recognized anticancer potential[13,14,15]. Such evidence positions Cissus verticillata as a promising candidate for detailed phytochemical and pharmacological investigations.

Modern phytochemical profiling technologies, particularly liquid chromatography coupled with high-resolution mass spectrometry (LC-HRMS), have revolutionized the identification of bioactive plant metabolites. LC-HRMS enables high sensitivity, accurate mass determination, and structural elucidation of compounds present in complex botanical extracts. By establishing a comprehensive metabolite profile, LC-HRMS provides the foundation for linking specific phytochemicals with biological activity[16,17,18]. In the case of Cissus verticillata, such profiling can uncover a wide array of flavonoids, phenolic acids, and tannins that are potential HER2 inhibitors.

While, modern computational approaches, including molecular docking and in silico ADMET (absorption, distribution, metabolism, excretion, and toxicity) analysis, have revolutionized drug discovery by enabling the prediction of ligand-receptor interactions, binding affinities, and pharmacokinetic profiles before experimental validation. Molecular docking allows for the virtual screening of phytochemicals against HER2, providing insights into potential binding modes, interaction energies, and critical amino acid residues involved in stabilization. Complementarily, ADMET analysis facilitates the evaluation of drug-likeness, bioavailability, and safety, ensuring that identified compounds possess favorable pharmacological properties[19,20,21,22]. Integrating these approaches with phytochemical profiling not only accelerates the identification of potential HER2 inhibitors but also reduces the time, cost, and risk associated with traditional drug discovery pipelines.

The convergence of traditional knowledge and computational pharmacology creates a robust platform for discovering novel therapeutics from plants. Cissus verticillata, with its ethnomedicinal background and phytochemical richness, represents an underexplored yet highly promising resource. Evaluating its metabolites against HER2 not only advances cancer research but also validates the scientific basis of traditional medicine. Furthermore, such research may contribute to the development of plant-based or plant-inspired drugs with reduced toxicity, lower costs, and improved accessibility compared with current HER2-targeted therapies.

Therefore, the present study is designed to explore Cissus verticillata as a potential source of HER2 inhibitors through a multi-tiered approach that integrates phytochemical profiling, molecular docking, and ADMET analysis. This comprehensive strategy aims to identify and evaluate key bioactive metabolites with dual emphasis on molecular efficacy and pharmacokinetic safety. By doing so, the research seeks to bridge the gap between traditional herbal knowledge and modern drug discovery, ultimately contributing to the global pursuit of safer and more effective cancer therapeutics.

MATERIALS AND METHODS

Collection of Plant Material and Authentication

Cissus verticillata herb was collected in the month of December 2024 from local area of Buldhana, Maharashtra, India. From the collected plant material, the herbarium was prepared and authenticated by Dr. K. Madhava Chetty, Head of Botanical Department of Sri Venkateswara University, Tirupati, 517502, Andhra Pradesh, India, on 28-12-2024. A voucher specimen no. 0211 was deposited. After collecting the authentication certificate, the extraction procedure was performed. The images of the plant are depicted in Figure 1.

Figure 1. The Cissus verticillata plant collected from XYZ District

Soxhlet Extraction using Hydroalcoholic Solvent

Leaves and bark of Cissus verticillata were collected, washed with distilled water to remove debris, and shade-dried at room temperature for a week to preserve volatile constituents. About 500 g of dried material was coarsely powdered and subjected to Soxhlet extraction using a hydroalcoholic solvent (ethanol:water, 70:30). The process continued for 24 hours, with repeated siphon cycles ensuring complete extraction of secondary metabolites, indicated by the fading of plant material and dark green color of the solvent. The extract was concentrated by natural evaporation in petri plates and stored for subsequent qualitative analysis[23,24,25,26].

Physicochemical and Phytochemical Evaluation

The hydroalcoholic extract was subjected to comprehensive physicochemical analysis, including assessment of colour, odour, and taste under natural conditions, as well as pH determination of 1% and 10% aqueous solutions using a digital pH meter. Foreign matter was separated and quantified, while moisture content was estimated by loss on drying (LOD) at 105 °C. Ash values were determined as total, acid-insoluble, sulphated, and water-soluble fractions, and extractive values were calculated for alcohol- and water-soluble components through maceration. Heavy metal estimation was carried out using microwave digestion followed by atomic absorption spectrometry, focusing on arsenic, cadmium, lead, mercury, zinc, copper, chromium, and manganese. Pesticide residue analysis was performed using GC with an electron capture detector, confirming absence of significant contamination[27,28].

Preliminary phytochemical screening of the crude extract was performed using standard qualitative assays. The tests confirmed the presence of carbohydrates, reducing sugars, monosaccharides, proteins, amino acids, fats and oils, steroids, glycosides, saponins, anthraquinones, flavonoids, tannins, phenolic compounds, alkaloids, and cyanogenetic glycosides. Specific reagents such as Molisch's, Fehling's, Benedict's, Biuret, Ninhydrin, Salkowski, Liebermann–Burchard, Keller–Killiani, Borntrager's, Shinoda, Dragendorff's, and ferric chloride were employed to establish metabolite identity. The results indicated abundant flavonoids and phenolics, moderate levels of tannins, glycosides, and saponins, and trace alkaloids, thereby validating the therapeutic potential of the extract[29,30,31,32,33].

Microbial Evaluation

The microbial content of the extracts was assessed using the pour plate method. For solid samples, 1 g of powder was dispersed in 9 mL sterile distilled water, while liquid samples were diluted similarly. Serial dilutions were prepared, plated on nutrient agar, cetrimide nutrient agar, salt nutrient agar, and MacConkey agar, and incubated at 37 °C for 24 h. Fungal growth was evaluated on Sabouraud dextrose agar plates incubated at 27 °C for 72 h. Colony forming units (CFU) were counted, and results were expressed as the mean of duplicate determinations[29,30,31,32,33].

Specific microbial contaminants were screened through enrichment and selective culture methods. Escherichia coli detection involved enrichment in nutrient broth followed by transfer to MacConkey broth and monitoring for acid and gas formation. Salmonella spp. were enriched in nutrient broth, transferred to selenite and tetrathionate broths, and streaked on deoxycholate citrate agar plates. Shigella spp. were enriched in nutrient broth (pH 8.0), plated on Salmonella–Shigella agar, and confirmed using Triple Sugar Iron (TSI) tests. Pseudomonas aeruginosa was isolated on soybean–casein digest medium, subcultured on cetrimide agar, and confirmed by oxidase testing. Staphylococcus aureus was enriched in peptone water, plated on Mannitol Salt Agar (MSA), and identified by colony morphology followed by catalase and coagulase tests[29,30,31,32,33].

LC-HRMS Analysis

For chemical profiling, the concentrated extract was prepared in methanol of HPLC grade, passed through a 0.22 µm membrane filter, and subjected to LC-HRMS. Separation was carried out on a C18 reverse-phase column (150 × 4.6 mm, 2.6 µm) using a mobile phase consisting of

acetonitrile and water, both supplemented with 0.1% formic acid. A gradient elution was maintained with a flow rate in the range of 0.3–0.5 mL/min. Mass spectrometric measurements were obtained under electrospray ionization in both positive and negative modes, scanning a mass-to-charge ratio (m/z) window from 50 to 1500. The system was tuned to maximize ionization efficiency by adjusting desolvation temperature, nebulizer gas flow, and source voltage. High-resolution full scans were followed by MS/MS fragmentation for further structural confirmation of the detected ions. The spectral data were processed with instrument software, and tentative identification of metabolites was achieved by comparison of accurate mass values, retention behavior, and fragmentation profiles with standard databases and published references[17,18,34].

Molecular Docking

To evaluate the potential of phytoconstituents from Cissus verticillata in targeting the HER2 (Human Epidermal Growth Factor Receptor 2) enzyme, an in silico molecular docking approach was employed. The 3D structures of selected phytochemicals were first drawn using ChemDraw and their corresponding 3D conformers were retrieved or optimized through PubChem. The target protein HER2 was obtained from the RCSB Protein Data Bank (PDB ID: 3RCD) and was prepared for docking by removing water molecules, heteroatoms, and co-crystallized ligands using Discovery Studio. Energy minimization and addition of polar hydrogens were also performed during protein preparation. The docking site was defined around the XYZ coordinates (13.047658, 1.810132, 28.168947), which corresponds to the active site of the HER2 receptor. Ligands were converted into the appropriate format and subjected to energy minimization using Open Babel integrated within PyRx (Python Prescription). Docking simulations were conducted using AutoDock Vina in PyRx, and the binding affinities were recorded. The best docked poses based on binding energy were visualized and analyzed using Discovery Studio Visualizer, focusing on hydrogen bonds, hydrophobic interactions, and other key receptor-ligand interactions to interpret binding mode and strength[19,20,21,22].

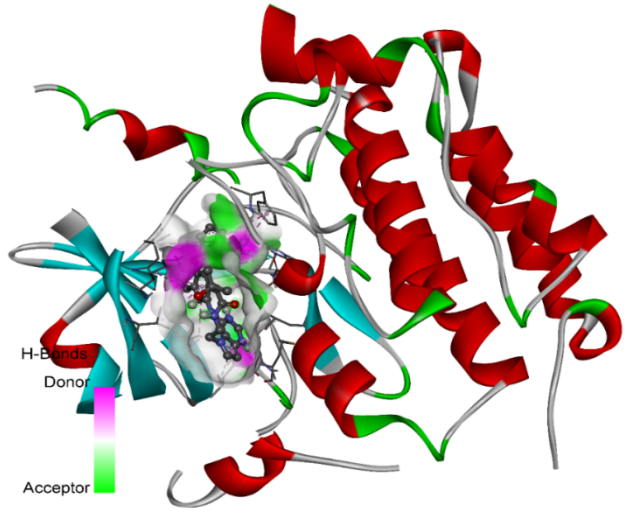

Figure 2. 3D ribbon presentation of HER2 enzyme (PDB ID: 3RCD) with native ligand

In Silico ADMET Analysis

For the assessment of pharmacokinetic and toxicity profiles of the selected phytoconstituents from Cissus verticillata, ADMET (Absorption, Distribution, Metabolism, Excretion, and Toxicity) analysis was performed using both SwissADME and ADMETlab 3.0 web-based platforms. The 2D chemical structures of the phytoconstituents were initially drawn using ChemDraw and their canonical SMILES (Simplified Molecular Input Line Entry System) notations were retrieved from PubChem. These SMILES strings were then input into SwissADME (http://www.swissadme.ch/) to predict key physicochemical properties, lipophilicity (logP), solubility (logS), pharmacokinetic parameters such as gastrointestinal (GI) absorption, blood-brain barrier (BBB) permeability, and drug-likeness based on Lipinski's Rule of Five. Additionally, ADMETlab 3.0 (https://admetlab3.scbdd.com/server/evaluation) was utilized to obtain a comprehensive prediction of ADME-related properties including P-glycoprotein substrate/inhibitor status, cytochrome P450 (CYP450) enzyme interactions, plasma protein binding (PPB), and toxicity endpoints such as hepatotoxicity, cardiotoxicity (hERG inhibition), and AMES mutagenicity. The combined output from both tools provided an in-depth understanding of the drug-likeness and safety profiles of the phytoconstituents, aiding in the selection of promising candidates for further drug development[19,20,21,22].

RESULTS AND DISCUSSION

Organoleptic, Physicochemical, Microbial, and Phytochemical Evaluation of Cissus verticillata Extract

Cissus verticillata was extracted using a hydroalcoholic solvent, yielding 10.95% extract with characteristic organoleptic properties. The extract appeared dark brown to greenish-brown, with a herbal, earthy, mildly bitter aroma, and a bitter, slightly astringent taste, consistent with phytochemical-rich botanicals. It exhibited a solid texture, indicating an efficient extraction process. Physicochemical analysis showed near-neutral pH values (7.2 for 1% solution and 6.9 for 10% solution), confirming stability and compatibility with biological systems (Figure 3). The extract contained no foreign matter, had a loss on drying of 6.5%, and ash values indicating moderate inorganic content: total ash (3.44%), acid-insoluble ash (0.12%), water-soluble ash (4.24%), and sulphated ash (2.32%). Extractive values revealed higher water solubility (13.25%) compared to alcohol solubility (8.97%), reflecting greater extraction of hydrophilic phytoconstituents. Importantly, no heavy metals or pesticide residues were detected, affirming its safety for pharmacological use. Microbial analysis confirmed the absence of pathogenic bacteria such as Escherichia coli, Salmonella spp., Shigella spp., Pseudomonas aeruginosa, and Staphylococcus aureus, ensuring microbiological safety and quality of the extract. Preliminary phytochemical screening revealed abundant alkaloids, flavonoids, and phenolic compounds (+++), indicating strong antioxidant, antimicrobial, and anti-inflammatory potential. Saponins and tannins were moderately present (++), while steroids and carbohydrates

were detected in trace amounts (+). Proteins, amino acids, fats and oils, anthraquinone glycosides, and cardiac glycosides were absent, suggesting the extract's bioactivity is primarily driven by secondary metabolites with targeted therapeutic potential (Figure 4).

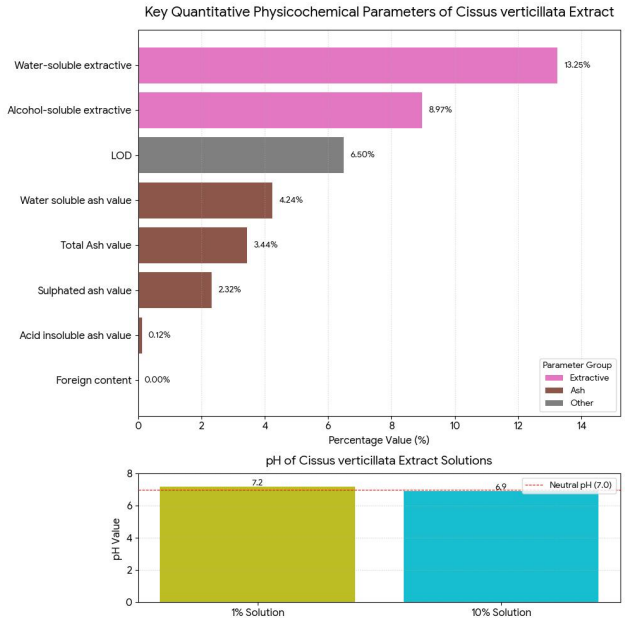

Figure 3. The physicochemical analysis of Cissus verticillata extract

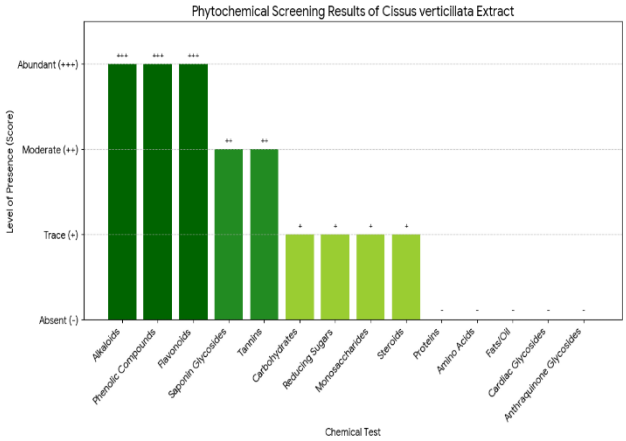

Figure 4. The results of preliminary phytochemical screening of Cissus verticillata extract

LC-HRMS Analysis

Chromatographic Profile

The LC-HRMS analysis of Cissus verticillata extract, produced a complex chromatographic fingerprint, reflecting the chemical diversity of the extract. The separation was achieved using an ACCUCORE C18 column (150 × 4.6 mm, 2.6 µm), and peaks were recorded in both positive and negative electrospray ionization (ESI) modes (Figure 5). Several well-defined peaks of varying intensities were observed across the retention time window, indicating the presence of multiple classes of phytochemicals. Key peaks with strong signals were selected for tentative identification.

Compound Identification

Accurate mass-to-charge ratios (m/z), retention times (RT), and literature-based fragmentation patterns were used to propose putative structures for the detected peaks. A total of seven compounds were tentatively identified (Table 1).

Flavonoid glycosides were represented by kaempferol-3-O-rutinoside (m/z 381.0; RT 1.45 min) and rutin (m/z 611.1; RT 4.28 min). These compounds showed typical fragmentation behavior associated with glycosylated flavonoids, including loss of sugar moieties.

Phenolic acids were highlighted by chlorogenic acid (m/z 341.1; RT 2.64 min), detected in both ionization modes. Its fragmentation matched well with caffeoylquinic acid derivatives commonly reported in plant tissues.

Condensed tannins were indicated by procyanidin B2 (m/z 681.4; RT 5.20 min), a dimeric flavanol frequently observed in bark and seed extracts.

Flavone glycosides such as luteolin-7-O-glucoside (m/z 433.1; RT 6.50 min) were identified, consistent with metabolites present in medicinal plants.

High-mass glycosides were represented by a saponin derivative (m/z 912.7; RT 8.52 min), with multiple adduct peaks suggestive of triterpenoid structures.

Polyphenolic complexes were observed at higher retention times, with a significant peak assigned to cinnamtannin A2 (m/z 1343.0; RT 13.50 min), indicative of oligomeric tannins.

Metabolite Classes

The distribution of compounds revealed the dominance of flavonoids, phenolic acids, tannins, and saponins, which are frequently associated with antioxidant, anti-inflammatory, and enzyme inhibitory activities. The early-eluting polar compounds (flavonoid glycosides and phenolic acids) were complemented by later-eluting high-mass metabolites (saponins and polyphenolic complexes), demonstrating a wide polarity range in the extract.

Table 1. Tentative identification of compounds detected by LC-HRMS

RT (min)	Observed m/z	Suggested Compound	Putative Class
1.45	381.0	Kaempferol-3-O-rutinoside	Flavonoid glycoside
2.64	341.1	Chlorogenic acid	Phenolic acid
4.28	611.1	Rutin	Flavonoid
5.20	681.4	Procyanidin B2	Tannin
6.50	433.1	Luteolin-7-O-glucoside	Flavone glycoside
8.52	912.7	Saponin derivative	Saponin
13.50	1343.0	Polyphenolic complex (Cinnamtannin A2)	Polyphenol

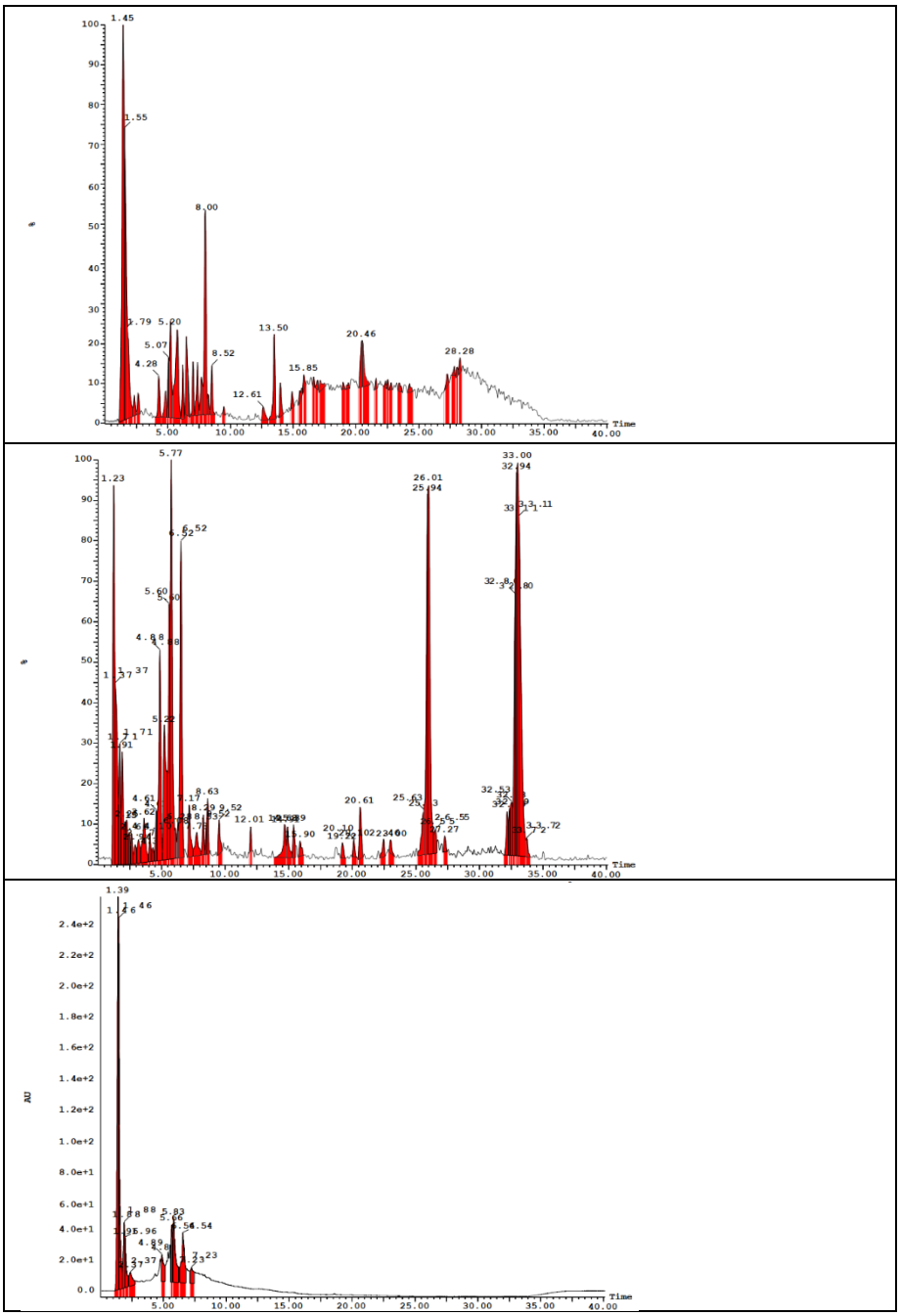

Figure 5. LC-HRMS graph of Cissus verticillata extract

Molecular Docking

The molecular docking analysis reveals valuable insights into the binding interactions between selected phytoconstituents from Cissus verticillata and the HER2 enzyme (PDBID: 3RCD) (Table 2). 2D and 3D interactions of all selected compounds and native ligand with HER2 enzyme are depicted in Table 3. The Native Ligand exhibits strong binding with HER2, forming conventional hydrogen bonds and halogen bonds with SER783 and GLN799. It also engages in various hydrophobic interactions, including pi-sigma, pi-pi T-shaped, alkyl, and pi-alkyl interactions with residues such as LEU785, PHE864, LEU800, and VAL734. The Native Ligand's docking score of -9.6 kcal/mol serves as a benchmark for comparing the phytoconstituents. Among the selected compounds, Kaempferol-3-O-rutinoside and Rutin demonstrate the most promising results. Kaempferol-3-O-rutinoside achieves a docking score of -10.2 kcal/mol, surpassing the Native Ligand. It forms multiple conventional hydrogen bonds with residues like MET801, ASP863, and ARG849, as well as hydrophobic interactions with LEU852, ALA751, and LYS753. Similarly, Rutin exhibits a high binding affinity with a docking score of -10.3 kcal/mol. It forms numerous hydrogen bonds with residues such as ASN850, ASP863, and LYS753, along with hydrophobic interactions involving LEU785, VAL734, and LEU796. Luteolin-7-O-glucoside also shows strong binding potential with a docking score of -9.9 kcal/mol. It forms conventional hydrogen bonds with MET801 and engages

in various hydrophobic interactions, including pi-pi stacked interactions with PHE1004 and pi-alkyl interactions with LEU726 and VAL734. Procyanidin B2 and Soyasaponin I display moderate binding affinities with docking scores of -9.2 kcal/mol and -9.1 kcal/mol, respectively. Both compounds form hydrogen bonds and hydrophobic interactions with key residues in the binding pocket. Chlorogenic Acid and Cinnamtannin A2 show lower binding affinities compared to the Native Ligand, with docking scores of -8.2 kcal/mol and -6.2 kcal/mol, respectively. While they still form hydrogen bonds and hydrophobic interactions, their overall binding strength appears to be weaker. These results suggest that Kaempferol-3-O-rutinoside, Rutin, and Luteolin-7-O-glucoside have the potential to be effective HER2 inhibitors, possibly surpassing the Native Ligand in binding affinity. The other compounds, while showing some degree of interaction, may be less effective as HER2 inhibitors based on their docking scores and interaction profiles. Further experimental studies would be necessary to validate these computational findings and assess the actual inhibitory potential of these phytoconstituents against HER2 in biological systems.

Table 2. Binding interactions of selected derivatives and Native Ligand with HER2 Enzyme (PDBID: 3RCD)

Amino acid residues	Bond Length	Bond Type	Bond Category	Ligand Energy (Kcal/mol)	Docking Score
Native Ligand					
SER783	2.77655	Hydrogen Bond;Halogen	Conventional Hydrogen Bond;Halogen (Fluorine)	561.27	-9.6
GLN799	3.64096	Hydrogen Bond	Carbon Hydrogen Bond		
SER783	3.43264	Halogen	Halogen (Fluorine)		
SER783	3.08629				
SER783	2.82107				
ARG784	3.57373				
LEU785	3.89967	Hydrophobic	Pi-Sigma		
PHE864	5.39098		Pi-Pi T-shaped		
LEU800	5.33502		Alkyl		
LEU852	4.36992				
LYS753	4.80989				
LEU796	5.09934				
LEU785	4.47644				
ALA751	4.60379				
VAL734	5.31832		Pi-Alkyl		
ALA751	5.21583				
LYS753	4.07798				
LEU796	4.99116				
UNK1:C	4.86076				
Chlorogenic_Acid					
ALA751 :O	2.13451	Hydrogen Bond	Conventional Hydrogen Bond	230.28	-8.2
LEU726	4.96872	Hydrophobic	Pi-Alkyl		
VAL734	5.47943				
LEU852	5.12581				
Cinnamtannin_A2					
VAL725	2.23827	Hydrogen Bond	Conventional Hydrogen Bond	1037.23	-6.2
ASP808	2.32853				
ARG849	2.20568				
ASN850	2.50023				
LYS753	2.98685				
ARG849	3.03988				
VAL884	2.44205				

CYS805	5.2688	Hydrophobic	Pi-Alkyl		
VAL734	5.1882				
ALA730	4.73576				
PRO885	4.6383				
Kaempferol-3-O-rutinoside					
MET801	1.88055	Hydrogen Bond	Conventional Hydrogen Bond	1599.42	-10.2
ASP863	2.78728				
ARG849	2.07279				
ASP863	2.30007				
ASP863	3.05892				
ARG849	2.04925				
ALA730	2.38374				
ARG849	2.44715				
GLY729	3.14433		Carbon Hydrogen Bond		
LEU852	3.50507	Hydrophobic	Pi-Sigma		
ALA730	3.45844		Alkyl		
ALA751	4.71515		Pi-Alkyl		
LYS753	5.24786				
ALA751	5.11662				
LYS753	4.30504				
ALA751	4.26947				
ALA730	5.24026				
Luteolin-7-O-glucoside					
MET801	2.77335	Hydrogen Bond	Conventional Hydrogen Bond	319.45	-9.9
ASP863	3.69383		Carbon Hydrogen Bond		
LEU852	3.74661	Hydrophobic	Pi-Sigma		
PHE1004	3.87714		Pi-Pi Stacked		
LEU726	5.21627		Pi-Alkyl		
ALA751	5.42524				
VAL734	4.85841				
ALA751	4.2873				
LEU852	4.57512				
LEU726	4.93258				
Procyanidin_B2					
LEU796	2.34407	Hydrogen Bond	Conventional Hydrogen Bond	499.63	-9.2
GLY727	3.17913		Carbon Hydrogen Bond		
LEU726	3.76185	Hydrophobic	Pi-Sigma		
THR79	3.81631				
PHE1004	5.55497		Pi-Pi T-shaped		
VAL734	5.29076		Pi-Alkyl		
VAL734	5.47377				
ALA751	4.21905				
LYS753	4.50061				
Rutin					

ASN850	2.40363	Hydrogen Bond	Conventional Hydrogen Bond	1639.89	-10.3
ASP863	2.36786				
ALA751	2.29176				
LYS753	2.79803				
LYS753	2.15333				
THR862	2.40721				
ASP863	2.68003				
LYS753	3.13897	Hydrogen Bond;Electrostatic	Pi-Cation;Pi-Donor Hydrogen Bond		
LEU785	3.5841	Hydrophobic	Pi-Sigma		
MET774	5.44337	Other	Pi-Sulfur		
VAL734	4.63331	Hydrophobic	Alkyl		
VAL734	5.39496		Pi-Alkyl		
ALA751	5.20926				
LYS753	4.44004				
LYS753	5.38806				
LEU796	4.97919				
LEU755	5.26911				
LEU796	5.14965				
VAL734	4.8341				
Soyasaponin_I					
ASP808	2.56155	Hydrogen Bond	Conventional Hydrogen Bond	945.03	-8.7
GLY727	2.09895				
ASP808	2.80786				
CYS805	2.8859				
LEU726	3.98585	Hydrophobic	Alkyl		
VAL734	3.41688				
ALA751	4.47922				
LEU852	4.0149				
VAL734	5.14519				
LYS753	4.09353				
LYS753	3.53843				
LEU796	4.96787				
LYS753	3.58389				
LEU796	3.41637				
ARG849	4.00182				
VAL734	4.01191				
VAL734	4.52965				
ALA751	4.77304				
ALA751	4.49664				
LYS753	4.52712				
CYS805	4.69447				
LEU852	5.32379				

Table 3. 2D and 3D interactions of all selected compounds and native ligand with HER2 enzyme.

3D Interactions	2D Interactions
Native Ligand	
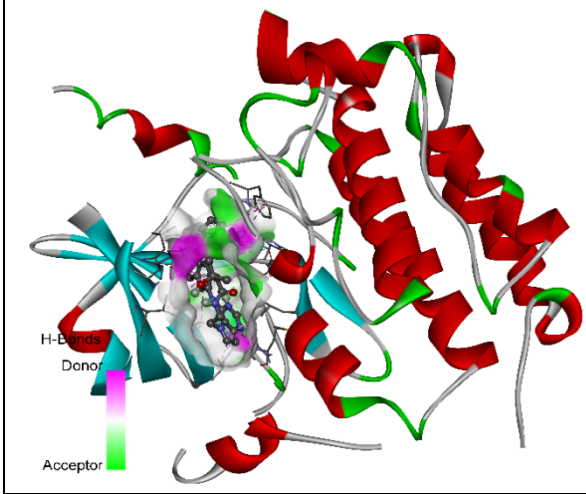	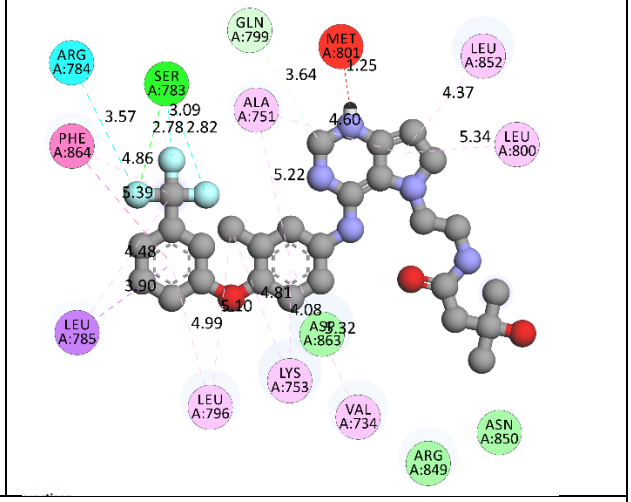
Chlorogenic_Acid	
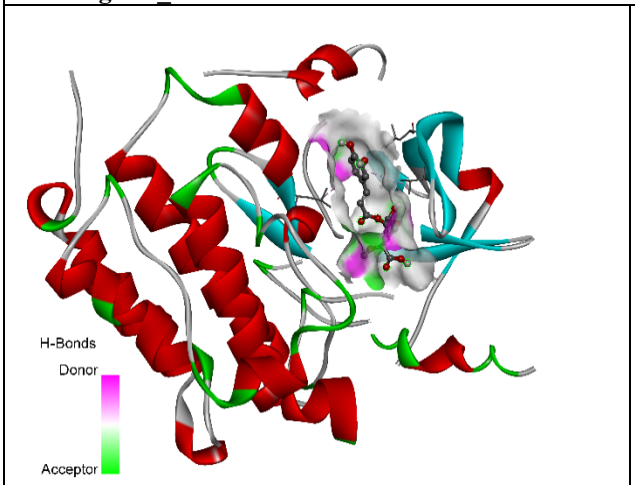	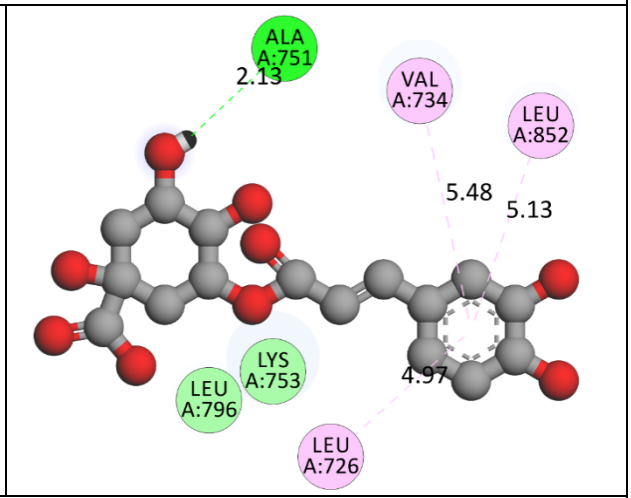
Cinnamtannin_A2	
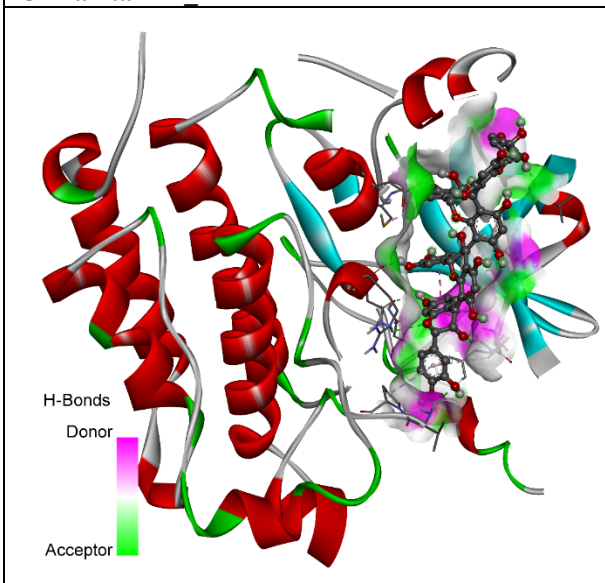	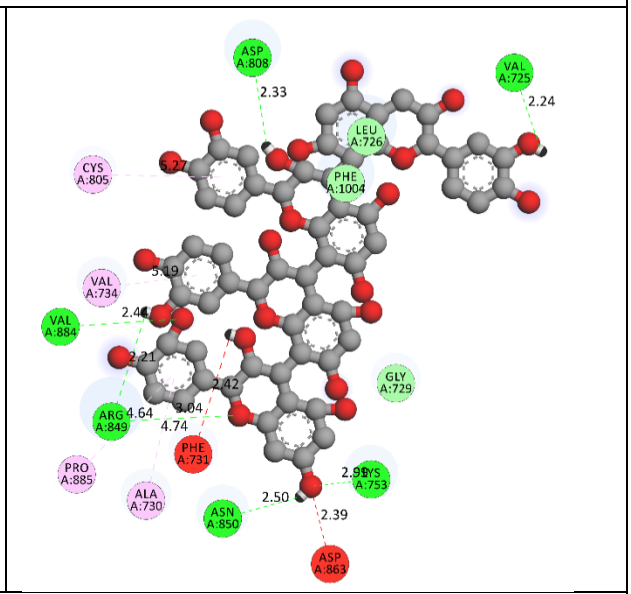
Kaempferol-3-O-rutinoside	

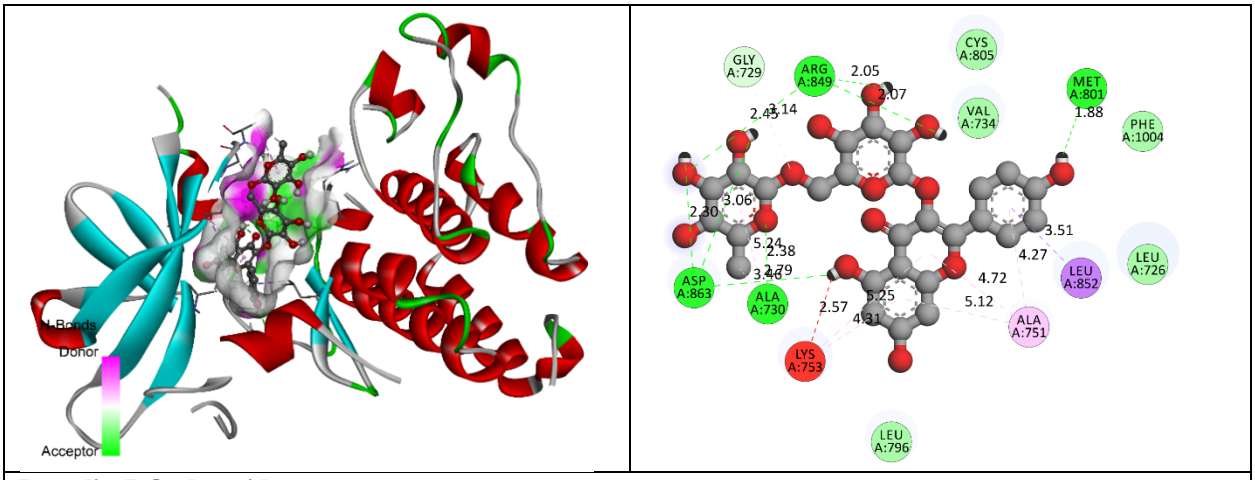

Luteolin-7-O-glucoside

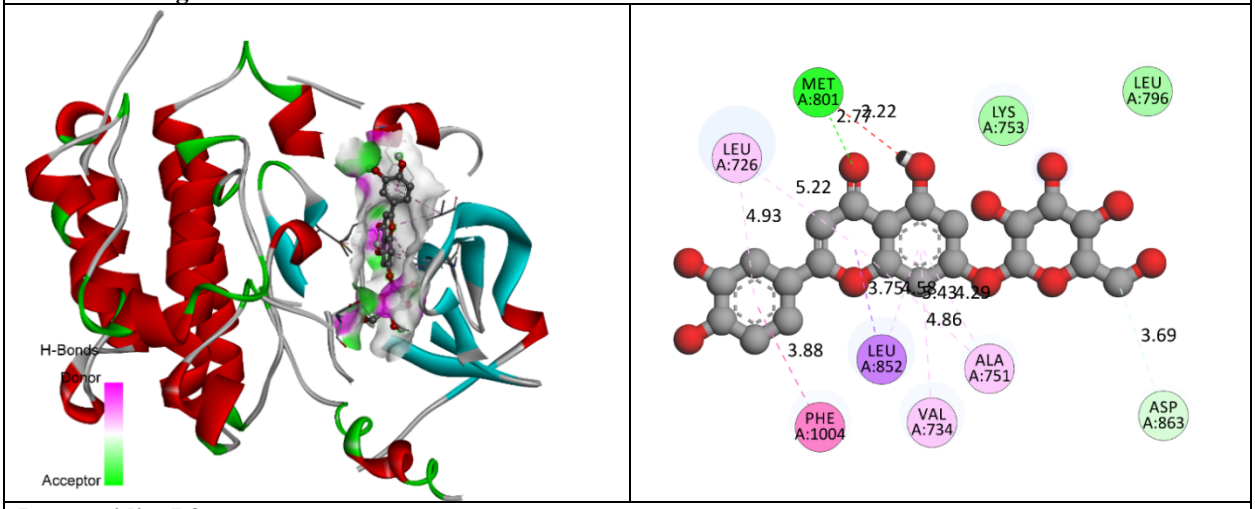

Procyanidin_B2

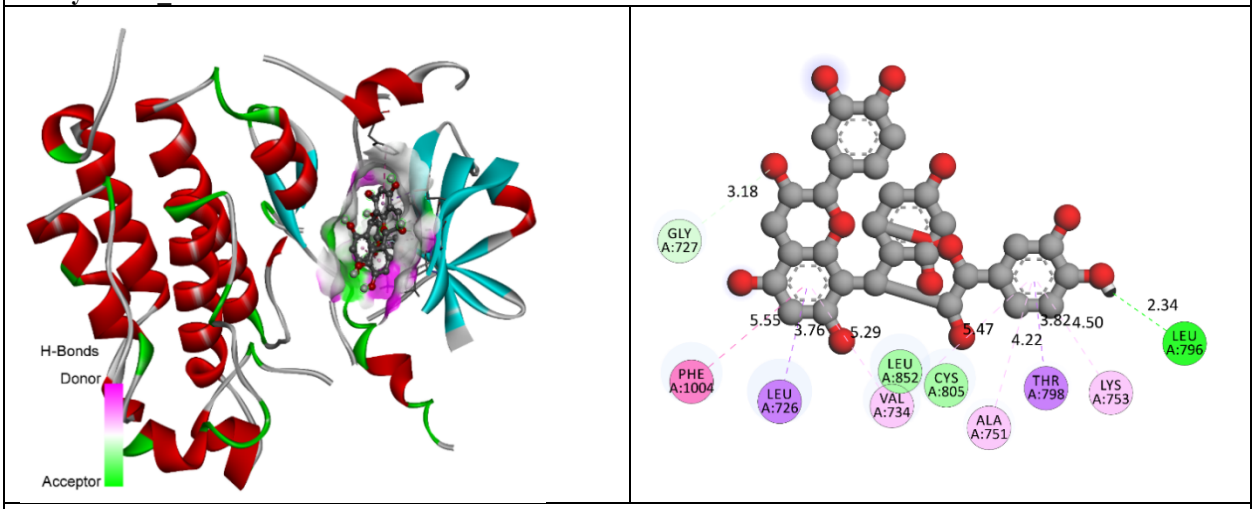

Rutin

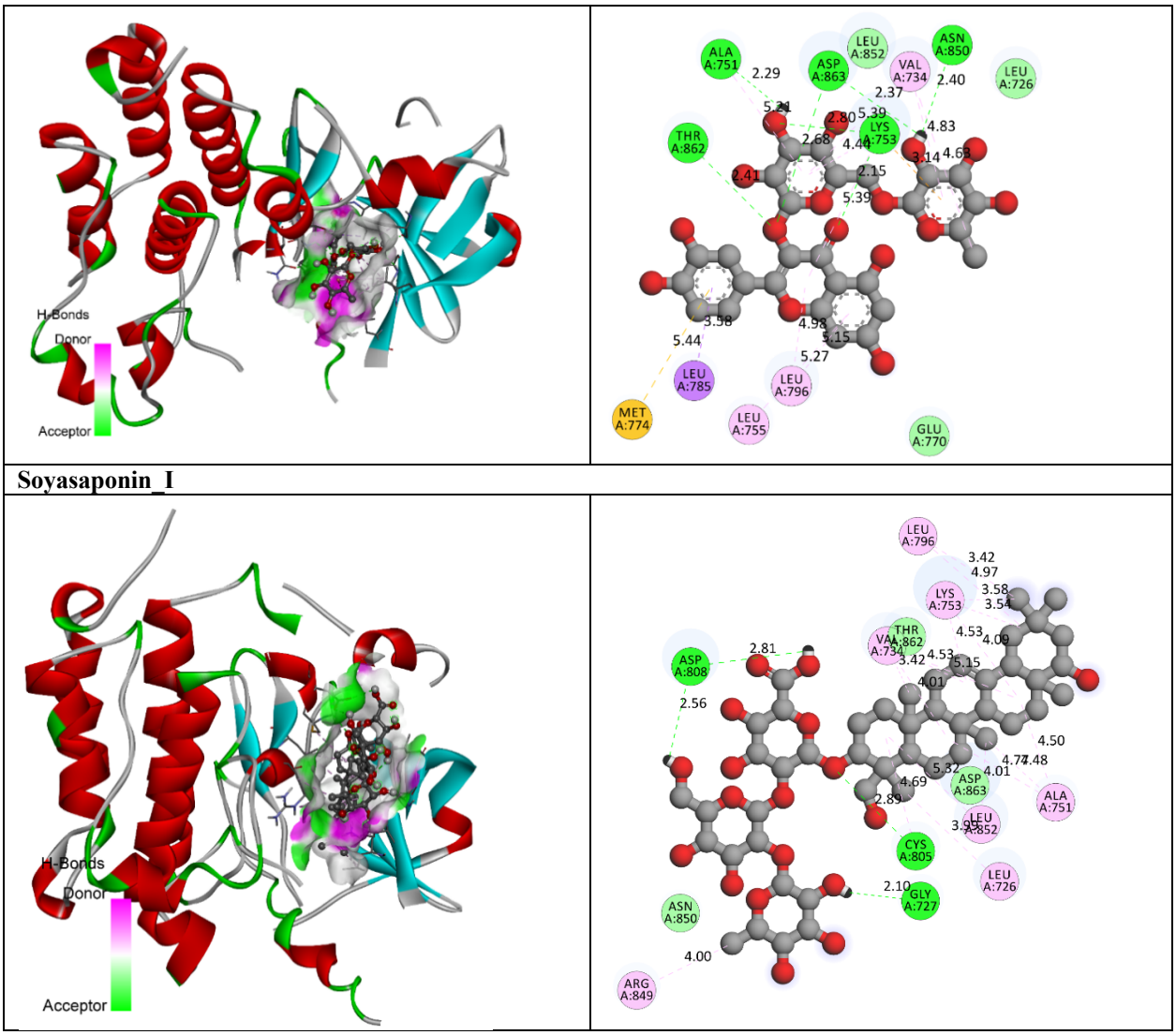

In Silico ADMET analysis

The comprehensive in silico ADMET evaluation of identified phytoconstituents from Cissus verticillata offers essential insights into their pharmacokinetic and toxicity characteristics pertinent to HER2-targeted medication development. The physicochemical properties that significantly affect absorption, distribution, and overall drug-likeness indicate that the native ligand has a high molecular weight (547.16 Da), increased lipophilicity (logP: 4.61), and low aqueous solubility (logS: -6.07), characteristics typically linked to inadequate oral bioavailability (Table 4). Conversely, some phytoconstituents—including chlorogenic acid, luteolin-7-O-glucoside, and kaempferol-3-O-rutinoside—demonstrate superior physicochemical properties, characterized by reduced molecular weights, enhanced solubility (logS values ranging from -2.5 to -3.6), and moderate lipophilicity (logP around 1.0). These characteristics signify enhanced oral drug-likeness and absorption capability. While molecules such as cinnamtannin A2 and soyasaponin I exhibiting elevated TPSA and molecular weight—attributes generally detrimental to passive permeability—their structural intricacy may enhance biological selectivity in some scenarios.

Assessments of drug-likeness further confirm the enhanced suitability of the phytoconstituents for oral delivery (Table 5). The native ligand does not meet the criteria specified by Pfizer and GSK, and exhibits a low QED score of 0.241, indicating inadequate drug-likeness. In contrast, phytoconstituents like chlorogenic acid and luteolin-7-O-glucoside have similar or superior QED values and elevated natural product (NP) scores (>1.9), indicating advantageous structural characteristics and possible biological significance. Despite the fact that the majority of phytochemicals contravene at least one Lipinski criterion—primarily owing to elevated hydrogen bond counts or molecule dimensions—they mostly adhere to the Golden Triangle and GSK principles, highlighting their satisfactory physicochemical equilibrium. The positive chelator rule seen in several flavonoid and polyphenolic substances indicates potential for metal ion interaction, which may be advantageous or harmful depending on the specific situation.

The absorption results indicate a significant drawback for the native ligand, exhibiting low intestinal permeability (Caco-2: -5.23) and very poor predicted human intestinal absorption (HIA: 0.022). However, soyasaponin I, rutin, and procyanidin B2 have elevated HIA values (>0.9) and substantial oral bioavailability across F20%, F30%, and F50% indices, signifying advantageous absorption properties. Chlorogenic acid has superior oral bioavailability with little P-glycoprotein substrate or inhibitory capacity, hence diminishing the likelihood of drug efflux. Cinnamtannin A2 has low membrane permeability; yet, its anticipated high oral bioavailability (F50% = 1.0) is significant, but somewhat deceptive owing to its molecular size and hydrogen bonding characteristics. The data indicate that certain phytoconstituents surpass the native ligand for expected absorption and bioavailability (Table 6).

The distribution and metabolism parameters further distinguish the substances (Table 7). The native ligand exhibits significant plasma protein binding (99.09%) and a constrained volume of distribution, suggesting limited tissue distribution. Conversely, chlorogenic acid and luteolin-7-O-glucoside exhibit reduced protein binding and elevated free drug fractions (Fu > 13%), enhancing target interaction. Furthermore, the native ligand has substantial interactions with cytochrome P450 enzymes, especially as a substrate for CYP3A4, thereby increasing the risk of drug-drug interactions and metabolic instability. In contrast, the majority of phytochemicals exhibit little CYP inhibition or substrate activity, resulting in reduced metabolic liability and enhanced predictability in pharmacokinetics. Procyanidin B2 and soyasaponin I exhibit little CYP interaction, hence improving their characteristics as metabolically stable options.

The native ligand exhibits high clearance and a short half-life (T½ = 0.54 h), indicating fast removal and perhaps necessitating regular administration. Furthermore, it has significant anticipated hepatotoxicity (0.89), propensity for drug-induced liver damage (0.97), and respiratory toxicity (0.86), making it less advantageous from a safety perspective. Conversely, phytoconstituents including chlorogenic acid and luteolin-7-O-glucoside exhibit markedly decreased toxicity profiles, encompassing less hepatotoxicity and mutagenicity, with enhanced safety regarding skin and ocular irritation. Cinnamtannin A2, despite its extended half-life (8.62 h) that may provide sustained pharmacodynamic benefits, demonstrates increased toxicity in some endpoints, requiring careful consideration. Rutin and kaempferol-3-O-rutinoside have satisfactory safety margins with little toxicity issues. The parameters of excretion and toxicity are shown in Table 8.

The environmental toxicity evaluation indicates that all chemicals are under tolerable bio-concentration limits, with BCF values below 1.5. The native ligand has moderate aquatic toxicity, but chlorogenic acid, kaempferol-3-O-rutinoside, and luteolin-7-O-glucoside have reduced environmental toxicity values (IGC50, LC50DM), therefore affirming their environmental compatibility (Table 9). This factor is especially significant for substances evaluated for extensive manufacturing and use. In summary, while the native ligand has advantageous HER2 binding affinity, its pharmacokinetic constraints and toxicity profile considerably restrict its developmental potential. Chlorogenic acid, luteolin-7-O-glucoside, and kaempferol-3-O-rutinoside are identified as the most promising candidates among the evaluated phytoconstituents because to their exceptional ADMET profiles. These compounds demonstrate excellent absorption, decreased toxicity, low metabolic interference, and minimum environmental impact, thus endorsing their promise as safer and more effective alternatives to the native ligand for HER2-targeted therapeutic applications. ADMET radar of all selected compounds with native ligand are shown in Table 10.

Table 4. Physicochemical properties of selected derivatives

Compounds	MW	Volume	Dense	nHA	nHD	nRot	nRing	TPSA	logS	logP
Native Ligand	547.16	509.7934	1.073297	8	3	11	4	101.3	-6.07271	4.609609
Chlorogenic Acid	354.1	331.4726	1.068263	9	6	5	2	164.75	-2.95844	1.035675
Cinnamtannin A2	1154.27	1091.328	1.057674	24	20	7	12	441.52	-4.52895	0.981993
Kaempferol-3-O-rutinoside	594.16	543.5275	1.093155	15	9	6	5	249.2	-2.55675	1.160389
Luteolin-7-O-glucoside	448.1	413.1471	1.084601	11	7	4	4	190.28	-3.66837	0.81243
Procyanidin B2	578.14	549.9425	1.051274	12	10	3	6	220.76	-3.31173	1.149859

Rutin	610.15	552.3177	1.104708	16	10	6	5	269.43	-2.39666	0.986122
Soyasaponin I	928.5	905.9673	1.024871	18	11	9	8	294.98	-3.87352	1.677957

Table 5. Drug-likeness properties of designed derivatives

Compounds	QED	NP Score	Lipinski Rule	Pfizer Rule	GSK Rule	GoldenTriangle	Chelator Rule
Native Ligand	0.241	-1.172	0	0	1	1	0
Chlorogenic Acid	0.234	2.246	0	0	0	0	1
Cinnamtannin A2	0.083	0.99	1	0	1	1	1
Kaempferol-3-O-rutinoside	0.159	1.945	1	0	1	1	0
Luteolin-7-O-glucoside	0.261	1.972	1	0	1	0	1
Procyanidin B2	0.159	1.929	1	0	1	1	1
Rutin	0.14	2.015	1	0	1	1	1
Soyasaponin I	0.11	2.312	1	0	1	1	0

Table 6. Absorption parameter of selected compounds

Compounds	Caco-2 Permeability	MDCK Permeability	Pgp-inhibitor	Pgp-substrate	HIA	F20%	F30%	F50%
Native Ligand	-5.23574	-5.08469	0.266528	0.636519	0.022941	0.371214	0.020962	0.997232
Chlorogenic Acid	-6.42616	-5.15807	2.56E-06	0.07899	0.106257	0.99152	0.995865	0.99921
Cinnamtannin A2	-8.68293	-4.64007	2.54E-11	0.017123	0	0.999965	1	1
Kaempferol-3-O-rutinoside	-6.53241	-5.0288	5.12E-07	0.923982	0.136693	0.157615	0.989903	0.99919
Luteolin-7-O-glucoside	-6.39352	-5.05448	4.86E-05	0.153041	0.469401	0.665784	0.997786	0.998747
Procyanidin B2	-7.22239	-4.86908	1.49E-06	0.084725	0.000367	0.997977	0.999981	0.999995
Rutin	-6.54652	-5.02701	6.22E-08	0.699256	0.639735	0.772111	0.999751	0.999936
Soyasaponin I	-6.14022	-5.21764	4.56E-12	0.193695	0.961041	0.898941	0.994859	0.999958

Table 7. Distribution and metabolism parameter of selected molecules

Compounds	Distribution				Metabolism									
					CYP1A2		CYP2C19		CYP2C9		CYP2D6		CYP3A4	
	PPB %	VD	BBB	Fu	Inhibitor	Substrate	Inhibitor	Substrate	Inhibitor	Substrate	Inhibitor	Substrate	Inhibitor	Substrate
Native Ligand	99.09294	0.273474	0.154844	0.429866	0.020557	0.393111	0.036818	0.007027	0.0195	0.000168	6.53E-05	0.000225	0.114765	0.999905
Chlorogenic Acid	64.83117	-0.011156	0.000187	31.62116	4.12E-09	4.07E-12	3.34E-06	1.01E-09	2.90E-07	0.003441	1.13E-06	5.51E-10	3.97E-08	6.88E-08
Cinnamtannin A2	87.07635	0.478333	3.13E-06	14.46499	6.23E-24	1	2.75E-05	0.625569	3.70E-11	0.022218	7.97E-33	1.03E-33	1.88E-15	2.13E-12
Kaempferol-3-O-rutinoside	85.11787	-0.03781	8.18E-05	13.38901	3.72E-05	0.006566	2.55E-06	1.59E-06	9.67E-06	0.000247	2.16E-05	4.18E-06	0.027368	1.93E-07
Luteolin-7-O-glucoside	79.34691	-0.00347	0.001926	18.42733	0.016175	0.000148	5.42E-07	3.21E-07	1.83E-05	0.003179	1.50E-05	0.009	0.01618	5.27E-07
Procyanidin B2	90.33684	0.269515	0.000494	17.46273	4.84E-11	0.999999	0.000129	0.022383	1.74E-07	0.637389	3.82E-15	3.39E-13	3.79E-08	2.60E-06
Rutin	85.0054	-0.05883	3.59E-05	14.65911	0.0001	0.00364	1.44E-07	1.07E-06	1.85E-06	7.47E-05	2.26E-06	1.48E-07	0.029205	2.29E-09
Soyasaponin I	67.48967	-0.46428	0.004134	21.59202	5.04E-17	5.27E-09	2.60E-13	0.000714	8.49E-09	8.03E-05	1.65E-09	4.06E-07	3.73E-07	2.24E-05

Table 8. Excretion and Toxicity parameters of selected compounds

Compounds	Excretion		Toxicity									
	CL-plasma	T1/2	H-HT	DILI	Ames Toxicity	Rat Oral Acute Toxicity	FDA MDD	Skin Sensitization	Carcinogenicity	Eye Corrosion	Eye Irritation	Respiratory Toxicity
Native Ligand	5.959764	0.545126	0.894356	0.97583	0.583268	0.370041	0.670105	0.362738	0.361974	1.09E-07	0.091755	0.868925
Chlorogenic Acid	3.339708	2.757687	0.542861	0.29109	0.386054	0.053934	0.409878	0.986365	0.22493	0.008178	0.841379	0.108553
Cinnamtannin A2	6.481594	8.626402	0.978416	0.995714	0.928488	0.949052	0.998436	1	0.000224	3.44E-14	0.10139	0.995427
Kaempferol-3-O-rutinoside	1.414836	4.271624	0.462769	0.914587	0.73364	0	0.148402	0.983965	0.079052	3.09E-05	0.894723	0.034867

Luteolin-7-O-glucoside	3.395733	3.971009	0.467227	0.952835	0.86855	0.071008	0.209427	0.99156	0.420677	5.41E-05	0.780003	0.067187	
Procyanidin B2	8.926722	3.979776	0.842384	0.7412	0.710891	0.744531	0.962248	0.999985	0.023725	3.41E-06	0.899264	0.954631	
Rutin	1.610724	4.616005	0.406325	0.936922	0.756376	0	0.137174	0.997444	0.046632	3.59E-05	0.904546	0.030272	
Soyasaponin I	0.004726	3.645359	0.712121	0.877409	0.381924	0	0.034616	0.999879	0.154816	8.17E-09	0.000753	0.009876	

Table 9. Environmental toxicity profile of designed molecules

Compounds	**BCF**	**IGC50**	**LC50FM**	**LC50DM**
Native Ligand	1.415082	3.764566	4.870027	5.500089
Chlorogenic Acid	0.419095	3.04556	3.936631	4.53114
Cinnamtannin A2	1.12316	4.178867	4.642563	5.264616
Kaempferol-3-O-rutinoside	0.561833	3.177655	3.798183	4.488873
Luteolin-7-O-glucoside	0.519126	3.144786	3.786586	4.583129
Procyanidin B2	1.177655	3.630484	4.187311	4.706862
Rutin	0.533413	3.180953	3.927314	4.680011
Soyasaponin I	0.894253	3.546674	4.140287	5.157055

Table 10. ADMET radar of all selected compounds and native Ligand

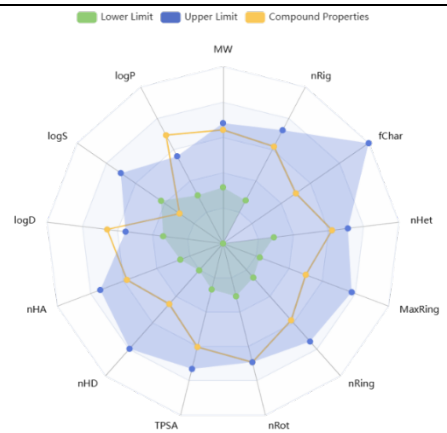

Native Ligand

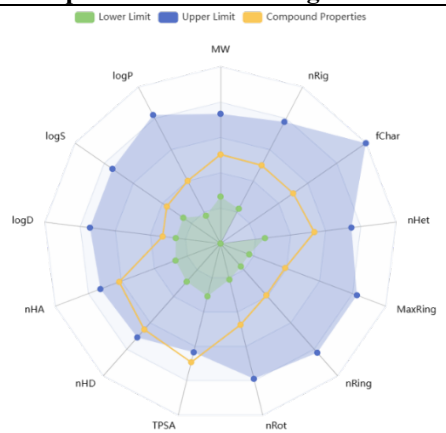

Chlorogenic Acid

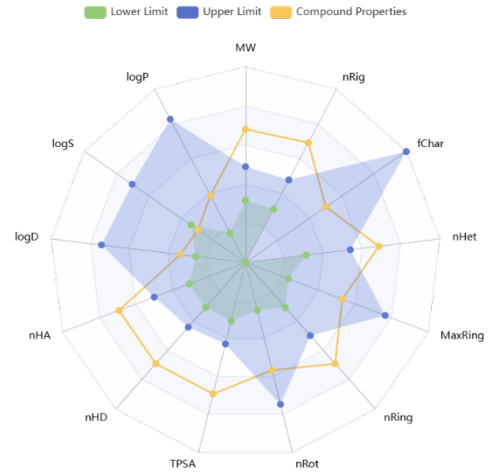

Cinnamtannin A2

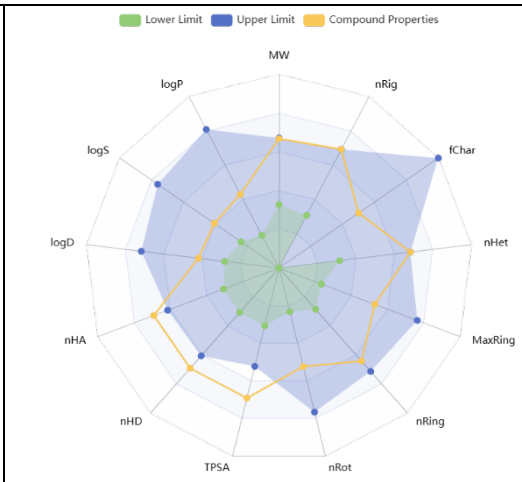

Kaempferol-3-O-rutinoside

Luteolin-7-O-glucoside

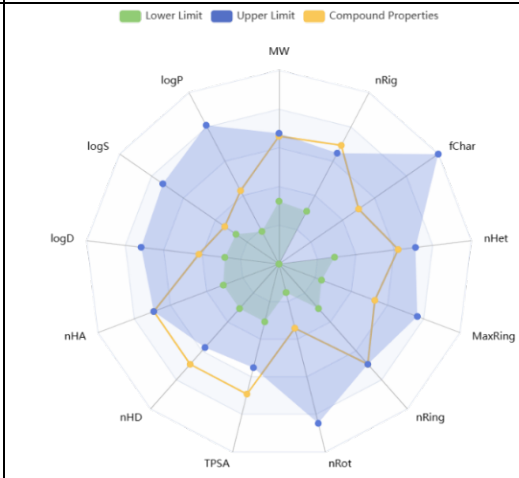

Procyanidin B2

Rutin

Soyasaponin I

CONCLUSION

In conclusion, the hydroalcoholic extract of Cissus verticillata demonstrated promising pharmacological potential, supported by its organoleptic, physicochemical, microbial, and phytochemical evaluations. The extract showed a stable physicochemical profile, absence of microbial contaminants, and a rich composition of bioactive secondary metabolites such as flavonoids, phenolic acids, tannins, and saponins. These findings establish the safety, quality, and therapeutic relevance of the extract. LC-HRMS profiling confirmed the presence of diverse phytochemicals, including kaempferol-3-O-rutinoside, rutin, chlorogenic acid, luteolin-7-O-glucoside,

procyanidin B2, a saponin derivative, and cinnamtannin A2. The identified compounds belong to major metabolite classes known for antioxidant, enzyme inhibitory, and anti-inflammatory activities, aligning with traditional uses of the plant. Molecular docking analysis revealed that kaempferol-3-O-rutinoside, rutin, and luteolin-7-O-glucoside possessed stronger HER2 binding affinities than the native ligand, suggesting their potential as effective HER2 inhibitors. In silico ADMET predictions further supported these compounds, indicating favorable absorption, reduced toxicity, minimal CYP450 interactions, and low environmental impact, whereas the native ligand exhibited poor pharmacokinetic and safety profiles. Overall, Cissus verticillata emerges as a phytochemical-rich candidate with significant therapeutic promise. However, further in vitro and in vivo studies are necessary to validate these computational and analytical findings and to advance its potential application in HER2-targeted therapy.

.

REFERENCES

1. Kulaksız T, Steinbacher J, Kalz M. Technology-enhanced learning in the education of oncology medical professionals: a systematic literature review. J Cancer Educ. 2023;38(5):1743–51.
2. Caballero D, Reis RL, Kundu SC. Cancer traps: implantable and on-chip solutions for early cancer detection and treatment. Adv Mater Technol. 2023;8(18):2300491.
3. Iqbal N, Iqbal N. Human epidermal growth factor receptor 2 (HER2) in cancers: overexpression and therapeutic implications. Mol Biol Int. 2014;2014:852748.
4. Budi HS, Ahmad FN, Achmad H, Ansari MJ, Mikhailova MV, Suksatan W, et al. Human epidermal growth factor receptor 2 (HER2)-specific chimeric antigen receptor (CAR) for tumor immunotherapy: recent progress. Stem Cell Res Ther. 2022;13(1):40.
5. Xie J, Zou Y, Gao T, Xie L, Tan D, Xie X. Therapeutic landscape of human epidermal growth factor receptor 2–positive breast cancer. Cancer Control. 2022;29:10732748221099230.
6. Alataki A, Dowsett M. Human epidermal growth factor receptor-2 and endocrine resistance in hormone-dependent breast cancer. Endocr Relat Cancer. 2022;29(8):R105–22.
7. Mueller V, Bartsch R, Lin NU, Montemurro F, Pegram MD, Tolaney SM. Epidemiology, clinical outcomes, and unmet needs of patients with HER2-positive breast cancer and brain metastases: a systematic review. Cancer Treat Rev. 2023;115:102527.
8. Atanasov AG, Waltenberger B, Pferschy-Wenzig EM, Linder T, Wawrosch C, Uhrin P, et al. Discovery and resupply of pharmacologically active plant-derived natural products: a review. Biotechnol Adv. 2015;33(8):1582–614.
9. Chaachouay N, Zidane L. Plant-derived natural products: a source for drug discovery and development. Drugs Drug Candidates. 2024;3(1):184–207.
10. Singla RK, Wang X, Gundamaraju R, Joon S, Tsagkaris C, Behzad S, et al. Natural products derived from medicinal plants and microbes as potential game-changers in breast cancer: a comprehensive review. Crit Rev Food Sci Nutr. 2023;63(33):11880–924.
11. Azab A, Nassar A, Azab AN. Anti-inflammatory activity of natural products. Molecules. 2016;21(10):1321.
12. Durazzo A, Lucarini M, Plutino M, Pignatti G, Karabagias IK, Martinelli E, et al. Antioxidant properties of bee products derived from medicinal plants. Agriculture. 2021;11(11):1136.
13. Paiva EA, Buono RA, Lombardi JA. Food bodies in Cissus verticillata: ontogenesis, structure and function. Ann Bot. 2009;103(3):517–24.
14. Kim W, Kwon HJ, Jung HY, Lim SS, Kang BG, Jo YB, et al. Cissus verticillata extract decreases oxidative stress–induced neuronal damage in HT22 cells and ischemia in gerbils. Plants. 2021;10(6):1217.
15. Drobnik J, de Oliveira AB. Cissus verticillata: identification and usage in sources from the 16th to 19th century. J Ethnopharmacol. 2015;171:317–29.
16. Aryal B, Adhikari B, Aryal N, Bhattarai BR, Khadayat K, Parajuli N. LC-HRMS profiling and antidiabetic, antioxidant and antibacterial activities of Acacia catechu. Biomed Res Int. 2021;2021:7588711.
17. Vasincu A, Luca SV, Charalambous C, Neophytou CM, Skalicka-Woźniak K, Miron A. LC-HRMS/MS profiling of Vernonia kotschyana: anticancer potential. S Afr J Bot. 2022;144:83–91.
18. Kızıltaş H, Bingol Z, Goren AC, Pınar SM, Alwasel SH, Gülçin İ. LC-HRMS profiling and bioactivities of Astragalus brachycalyx extract. —Journal details incomplete—.
19. Tamboli AS, Tayade SD. In-depth computational investigation of berberine and tropane as potential DPP-IV inhibitors for T2DM. J Pharm Sci Comput Chem. 2025;1(1):1–1.
20. Siddiqui F, Makhloufi R, Salah ME, Mohamed E, Hojjati M. Computational exploration of quinine and mefloquine as potential antimalarial agents. J Pharm Sci Comput Chem. 2025;1(2):106–15.
21. Ahmed SA, Tabassum PS, Falak SA, Ahmad AV, Shaikh MS. Molecular docking and network pharmacology of Vitis vinifera phytoconstituents against breast cancer. J Pharm Sci Comput Chem. 2025;1(2):116–34.
22. Jadhav SS, Dighe PR. In vitro evaluation and molecular docking of novel pyrazoline derivatives. J Pharm Sci Comput Chem. 2025;1(3):190–209.

23. Sharma V, Janmeda P. Extraction, isolation and identification of flavonoids from Euphorbia neriifolia. Arab J Chem. 2017;10(4):509–14.
24. Nickavar B, Mojab F, Javidnia K, Amoli MA. Chemical composition of fixed and volatile oils of Nigella sativa from Iran. Z Naturforsch C. 2003;58(9–10):629–31.
25. Talreja T, Kumar M, Goswami A, Gahlot G, Jinger SK, Sharma T. HPLC analysis of saponins in Achyranthes aspera and Cissus quadrangularis J Pharmacogn Phytochem. 2017;6(1):89–92.
26. Sahithi A, Mohan Chinala K, Chaithanya A, Achyuth Reddy C, Sawrov M, Al Amin M. Phytochemical and antimicrobial evaluation of Laurus nobilis leaves. J Pharm Sci Comput Chem. 2025;1:50–7.
27. Singh M, Tamboli ET, Kamal YT, Ahmad W, Ansari SH, Ahmad S. Quality control and antioxidant potential of Coriandrum sativum. J Pharm Bioallied Sci. 2015;7(4):280–3.
28. Kamal Y, Singh M, Salam S, Ahamd S. Standardization of Unani polyherbal formulation Qurse-e-Hummaz. Drug Dev Ther. 2016;7(1):39–45.
29. Khandelwal K. Practical Pharmacognosy. Pune: Pragati Books; 2008.
30. Mukherjee PK. Quality Control of Herbal Drugs: An Approach to Evaluation of Botanicals. New Delhi: Business Horizons; 2002.
31. Chaudhari RN, Khan SL, Chaudhary RS, Jain SP, Siddiqui FA. β-Sitosterol from Muntingia calabura: molecular docking as SARS-CoV-2 Mpro inhibitor. Asian J Pharm Clin Res. 2020;13:204–9.
32. Indrayanto G. Recent developments in quality control methods for herbal drugs. *Nat Prod Commun. 2018;13(12):1934578X1801301208.
33. Al-Busaid MM, Akhtar MS, Alam T, Shehata WA. Development and evaluation of herbal cream containing curcumin. Pharm Pharmacol Int J. 2020;8(5):285–9.
34. Luca SV, Minceva M, Gertsch J, Skalicka-Woźniak K. LC-HRMS/MS-based phytochemical profiling of Piper spices: association of piperamides with endocannabinoid modulation. Food Res Int. 2021;141:110123
.